METHOD FOR CONTROLLING A MULTI-DOF ULTRASONIC MOTOR USING A SIGMOID FUNCTION

Kenjiro Takemura* and Takashi Maeno**

* *Graduate School of Science and Technology, Keio University, 3-14-1 Hiyoshi, Kohoku-ku, Yokohama, 223-8522 JAPAN*

** *Department of Mechanical Engineering, Keio University, 3-14-1 Hiyoshi, Kohoku-ku, Yokohama, 223-8522 JAPAN*

ABSTRACT

A multi-degrees-of-freedom (DOF) ultrasonic motor developed by the authors generates rotations of a spherical rotor around three perpendicular axes using three natural vibrations of a bar-shaped stator. A method is proposed for controlling the multi-DOF ultrasonic motor. First, theoretical background of the ultrasonic motor is briefly described. Second, characteristics of the motor are measured precisely. Next, a method for controlling the multi-DOF ultrasonic motor, in which a phase difference is operated using a sigmoid function, is proposed. Then, the motion of the rotor around single-axis is controlled using the proposed method. Finally, the control method is applied to the multi-DOF motion of the rotor, and the appropriateness of the proposed method is confirmed.

1. INTRODUCTION

Needs for multi-DOF motion units are significantly increasing as the use of robotics technology is extending to many fields. However, general electromagnetic motors have only single-DOF motion, which result in increase of the total volume and weight of the multi-DOF motion unit. Hence, the expectation for multi-DOF actuators is increasing. A number of different actuators capable of generating multi-DOF motion have been developed or proposed in recent years [1].

Roth *et al.* proposed a three-DOF variable reluctance spherical wrist motor [2]. Yano developed a spherical stepping motor [3]. These motors use the principle of the electromagnetic motor, and therefore, geometries of the motors are complicated.

On the other hand, ultrasonic motors have excellent characteristics such as high torque at low speed, high stationary limiting torque, absence of electromagnetic radiation and simplicity of design. Therefore, multi-DOF actuators extending the principle of ultrasonic motors are proposed as follows.

Bansevicius developed a piezoelectric multi-DOF actuator [4] consists of a cylindrical stator (vibrator) and a spherical rotor. Amano *et al.* developed a multi-DOF ultrasonic actuator [5] in which a spherical rotor rotates around three perpendicular axes. Toyama constructed a spherical ultrasonic motor [6] consists of three ring-shaped stators and a spherical rotor. Sasae *et al.* developed a spherical actuator [7] where a three-DOF motion unit is constructed using truss arranged PZTs.

Although the actuators [4]-[7] can generate multi-DOF motion of the rotors, they cannot be used in place of multi-DOF motion units consists of general electromagnetic motors because of their small output torque, low controllability and non-simplicity of design. In order to solve these issues, the geometries of multi-DOF ultrasonic motors must be designed precisely.

The authors have developed a new type of ultrasonic motor capable of generating multi-DOF motion [8]. The multi-DOF ultrasonic motor generates multi-DOF rotation of a spherical rotor using three natural vibration modes of a bar-shaped stator.

Adopting the multi-DOF ultrasonic motor to practical applications, new control method for the motor must be proposed. There are several researches with respect to the motion controls for the ultrasonic motors. Senjyu *et al.* proposed a position control method of the ultrasonic motor using variable structure type adaptive control [9]. Lin *et al.* proposed fuzzy neural networks for identification and control of the ultrasonic motor drive [10]. In the control methods, modern control or intelligent control theory are used to deal with the difficulties of motion controls of ultrasonic motors. However, the reported researches focused on ring-shaped ultrasonic motors having single-DOF rotation. It is impossible to apply them to the multi-DOF ultrasonic motor developed by the authors, because the driving characteristic of the multi-DOF ultrasonic motor is complicated. Hence, a control method for the multi-DOF ultrasonic motor is proposed in this study.

In the present paper, the principle and geometry of the multi-DOF ultrasonic motor are briefly described in chapter 2. The driving characteristics of the multi-DOF ultrasonic motor are described in chapter 3. Then, proposed control methods for the multi-DOF ultrasonic motor are shown in chapter 4. The experimental results of the motion control tests are shown in chapter 5. Then in chapter 6, the conclusions of this study are described.

2. THEORETICAL BACKGROUND

We produced a multi-DOF ultrasonic motor in our previous study [8]. The driving principle and geometry of the ultrasonic motor are briefly described as follows.

2.1 Driving Principle

The multi-DOF ultrasonic motor we developed in our previous study consists of a bar-shaped stator and a spherical rotor. The spherical rotor rotates around three perpendicular axes by combining a first longitudinal vibration mode and two second bending vibration modes of the bar-shaped stator. Figure 1 shows the driving principle of the multi-DOF ultrasonic motor. The *x*-, *y*- and *z*-coordinate used in the present paper are defined as shown in Fig. 1.

Figure 1 (a) shows the case when the rotor rotates around the *z*-axis. When the second bending modes in the *z*-*x* and the *y*-*z* plane, illustrated in (i)(iii) and (ii)(iv), respectively, are combined at a phase difference of 90 deg, a point on the stator head draws an elliptic locus around the *z*-axis. Then, the rotor, in contact with the stator head, rotates around the *z*-axis by frictional force. Figure 1 (b) shows the case when the rotor rotates around the *x*-axis. When the first longitudinal mode along the *z*-axis and the second bending mode in the *y*-*z* plane, illustrated in (i)(iii) and (ii)(iv), respectively, are combined at a phase difference of 90 deg, a point on the stator head draws an elliptic locus around the *x*-axis. Then, the rotor rotates around the *x*-axis by frictional force. In case when the rotator rotates around the *y*-axis, the first longitudinal modes along the *z*-axis and the second bending mode in the *z*-*x* plane are combined in the same way as Fig. 1 (b). An important thing to be mentioned is that the natural frequencies of the first longitudinal mode and the second bending modes must almost correspond.

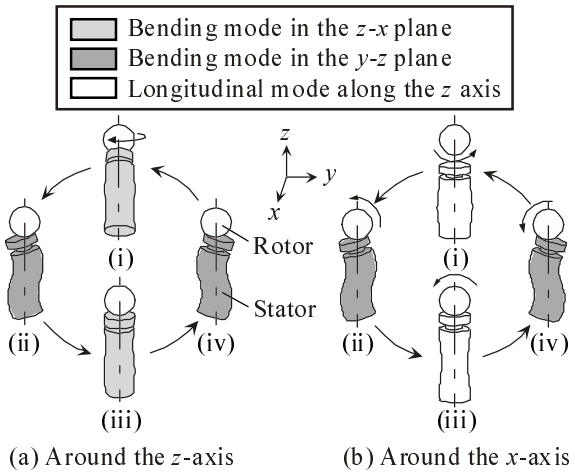

Fig. 1 Driving principle of a multi-DOF ultrasonic motor

2.2 Geometry

The natural frequencies of the first longitudinal and the second bending vibration modes must correspond as mentioned in the section 2.1. Hence, the geometry of the bar-shaped stator was designed using finite element analysis.

Figure 2 shows the multi-DOF ultrasonic motor we developed in our previous study (diameter and height of the stator are 10 and 31.85 mm, respectively). The spherical rotor is made of stainless steel. The bar-shaped stator mainly consists of brass head and rings, piezoelectric ceramic rings and a stainless steel shaft. The shaft is screwed up into the head in order to construct the stator as Langevin type vibrator. The piezoelectric ceramic rings are used to excite both the first longitudinal mode and the second bending modes of the bar-shaped stator. A cross-shaped phosphor bronze plate is fixed on to a pedestal, not illustrated in Fig. 2, in order to support the stator.

The natural frequencies of the first longitudinal mode and the second bending modes of the stator almost correspond. The experimental natural frequencies are around 40 kHz.

3. CHARACTERISTICS

The spherical rotor of the multi-DOF ultrasonic motor can rotate around three perpendicular axes [8]. In order to make the multi-DOF ultrasonic motor practical, the motion of rotor must be controlled so as to rotate around any axis. According to this, it is important to examine the driving characteristics of the multi-DOF ultrasonic motor. In this chapter, the driving characteristics around the *x*-axis are measured (*cf.* Fig. 1 and Appendix) to compare the effects of operating parameters such as frequency, voltage and phase difference. These are described in section 3.1, 3.2 and 3.3, respectively. The output torque is shown in section 3.4.

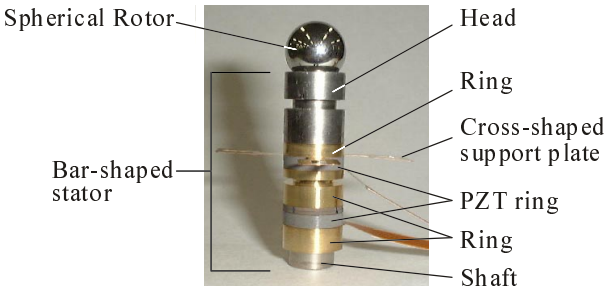

Fig. 2 The multi-DOF ultrasonic motor

3.1 Measured Relationship between Frequency and Rotational Speed

The measured relationship between the frequency and the rotational speed is shown in Fig. 3 (a). The frequency of the input signals was swept from 43 to 38 kHz. The voltages of the input signals for exciting the first longitudinal mode and the second bending mode were 20 and 40 $V_{p\text{-}p}$, respectively. The phase difference of them was 90 deg. The normal load between the stator and the rotor was 6 N.

It is seen from Fig. 3 (a) that the maximum rotational speed is obtained when the frequency of the input signals is about 40 kHz, which represents the natural frequencies of the first longitudinal mode and the second bending mode. Although the rotational speed can be varied by changing the frequency of the input signals, it is difficult to control the rotational speed linearly, because the relationship between the frequency and the rotational speed has a highly non-linear characteristic.

3.2 Measured Relationship between Voltage and Rotational Speed

The measured relationship between the voltage and the rotational speed is shown in Fig. 3 (b). Only the voltage of the input signal for the second bending mode was varied from 0 to 80 $V_{p\text{-}p}$, because the longitudinal vibration is mainly used as a clutch and does not provide much driving force. The experimental conditions, apart from the frequency of the input signals, were the same as those in the section 3.1. The frequency of the input signals was 39.28 kHz.

As can be seen from Fig. 3 (b), rotational speed changes almost linearly as the input voltage changes. The rotor does not stop when the voltage is 0 V, because the contact points between the rotor and the stator do not vibrate exactly along the *z*-axis when the first longitudinal mode is only excited on the stator.

3.3 Measured Relationship between Phase Difference and Rotational Speed

The measured relationship between the phase difference and the rotational speed is shown in Fig. 3 (c). Only the phase of the input signal for the second bending mode was varied and that for the first longitudinal mode was fixed at 0 deg. The experimental conditions except for the frequency of the input signals were the same as those in the section 3.1. The frequency of the input signals was 39.35 kHz. The positive and negative values of the rotational speed correspond to the rotational direction of the rotor, CW and CCW, respectively. Although the relationship between the phase difference and the rotational speed has a highly non-linear characteristic, the rotational speed can be varied by changing the phase difference of input signals. In addition, it can be seen that the rotational direction of the rotor can be reversed continuously by changing the sign of the phase difference.

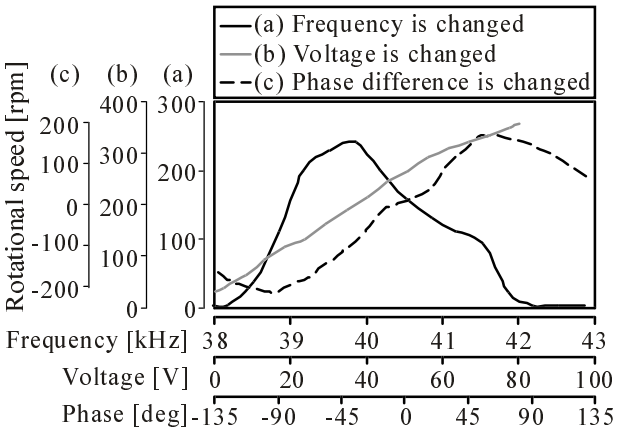

Fig. 3 Motor characteristics

3.4 Measured Relationship between Torque and Rotational Speed

Figure 4 shows the measured relationship between the torque and the rotational speed when the normal load between the stator and the rotor is varied. The experimental conditions, instead of the frequency of the input signals, were the same as those in the section 3.1. The frequency of the input signals was equal to the natural frequencies of the first longitudinal mode and the second bending mode of the stator.

It can be seen from Fig. 4 that the rotational speed decreases as the torque increases, and that the maximum torque increases as the normal load between the stator and the rotor increases. The maximum values of the rotational speed and the output torque under the experimented conditions are about 250 rpm and 7 mNm, respectively. The estimated rotational speed, calculated using the result of finite element analysis is about 400 rpm, and the estimated torque, calculated from the experimented conditions, is 20 mNm. The differences between the estimated and measured values are due to the followings.

The estimated values are calculated under the assumption that there are no stiffness and no slip state at the contact interface on the stator. However, at the contact interface, the rotor actually declines with respect to the stator, and there can be seen the stick/slip state. The difference causes the declinations as mentioned above [11][12]. In addition, the coefficient of friction under the ultrasonic

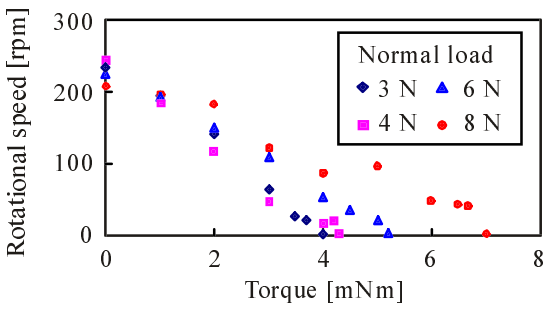

Fig. 4 Relationship between torque and rotational speed

vibration becomes lower than that under normal contact condition [13].

4. CONTROL METHOD

Control methods for the multi-DOF ultrasonic motor are proposed in this chapter. First, an operating parameter for the multi-DOF ultrasonic motor is determined considering the driving characteristics mentioned above. Then, a speed control method and a position control method are proposed. The rotor's rotation around single-axis is considered in the following discussion, although the proposed methods can be used when the rotational axis is extended to three perpendicular axes.

4.1 Operating Parameter

It is seen from Fig. 3 that the frequency, voltage and phase difference of input signals have potentials as operating parameters for controlling the motion of the multi-DOF ultrasonic motor. However, in case of the multi-DOF ultrasonic motor, we should determine its operating parameter considering the following requirements:

(i) The rotational speeds around the three perpendicular axes can be varied independently.
(ii) The vibration characteristics of the stator, such as natural frequencies, do not change even when the value of the operating parameter is changed.

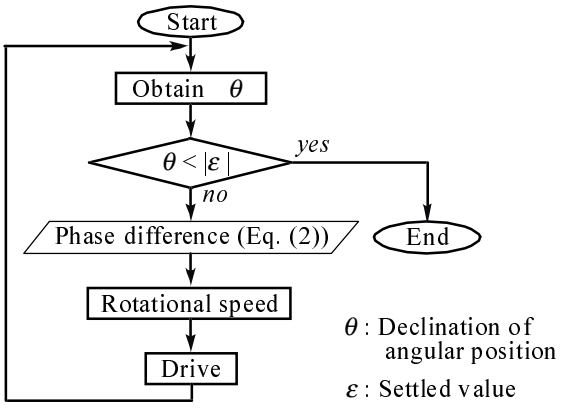

Fig. 5 Position control algorithm

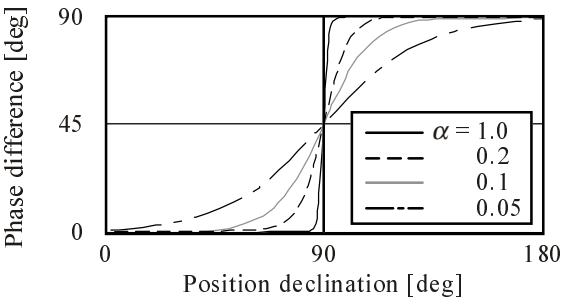

Fig. 6 Relationship between position declination and phase difference (sigmoid function)

(iii) The rotational direction can be changed.

With respect to the requirement (i), the frequency of input signals is not a suitable operating parameter for the multi-DOF ultrasonic motor because the rotational speed around the three perpendicular axes cannot be varied independently when the frequency is varied. Due to the requirement (ii), the voltage of input signals cannot be varied as operating parameters because the vibration characteristics of the natural vibrating modes, which have different modal masses and modal stiffness, change independently. Besides, it can be seen from Fig. 3 that the parameters except for the phase difference cannot meet the requirement (iii).

From the above discussion, we conclude that the phase difference of the input signals is a suitable operating parameter for the multi-DOF ultrasonic motor.

4.2 Speed Control Method

The rotational speed and rotational direction of the rotor can be varied by changing the phase difference of input signals as shown in Fig.3 (c). Hence, the rotational speed including the rotational direction can be controlled using a proportional controller as shown in the following equation, provided that the absolute value of phase difference is within 90 deg:

$$\Delta\phi = K_p \cdot \Delta N \tag{1}$$

where, $\Delta\phi$ is the phase difference, ΔN is the declination of rotational speed and K_p is the proportional feedback gain.

4.3 Position Control Method

A proposed position control algorithm is shown in Fig. 5. The rotational speed must be varied according to the declination of the angular position of the rotor, in order to make the response time short. Hence, The following sigmoid function is used to make the phase difference

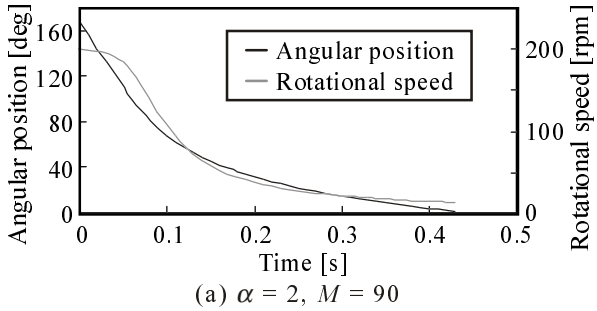

(a) α = 2, M = 90

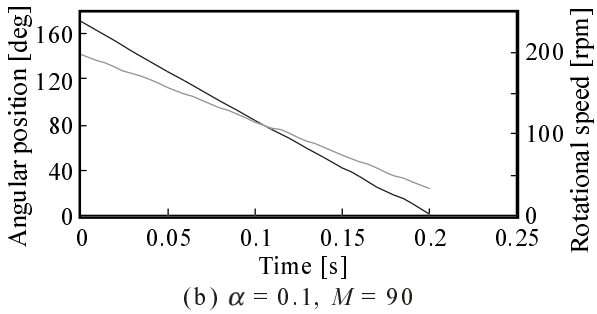

(b) α = 0.1, M = 90

Fig.7 Simulated step response of angular position

vary according to the declination of rotor position:

$$|\Delta\phi| = 90 \cdot \frac{1}{1+\exp(-\alpha(\Delta\theta - M))} \quad (2)$$

where, $\Delta\phi$ is the phase difference, $\Delta\theta$ is the declination of the angular position, and α and M are the parameters of the sigmoid function. The rotational speed becomes large because the declination of the angular position becomes large when the sigmoid function is used for control. Furthermore, the relationship between the declination and the phase difference can be easily varied changing the sigmoid function parameters α and M, as shown in Fig. 6. An efficiency of the method is confirmed using a computer simulation. The relationship between the phase difference and the rotational speed shown in Fig. 3 (c) is defined approximately using a sinusoidal function as follows:

$$N(\phi) = N_{\max} \cdot \sin\Delta\phi \quad (3)$$

where, N is the rotational speed, and $\Delta\phi$ is the phase difference. Simulated step responses of the angular position around the x-axis are illustrated in Fig. 7. The angular position is varied from 180 to 0 deg. It is seen from Fig. 7 that the control characteristic can be easily varied changing the sigmoid function parameter α.

5. MOTION CONTROL

Experimental results for motion control of the rotor using the control method proposed in the chapter 4 are shown as follows (*cf.* Appendix).

5.1 Experimental Results for Speed Control around Single-axis

The step response of the rotational speed was measured. The desired rotational speed was 200 rpm. The voltage of the input signals for the second bending mode and the first longitudinal mode were 40 and 20 $V_{p\text{-}p}$, respectively. The frequency of the input signals was 39.28 kHz. The phase difference between them was varied from –90 to 90 deg by Eq. (1).

Figure 8 shows the experimental results for the step response of the rotational speed when the proportional feedback gain is 0.1. It can be seen from Fig. 8 that the rotational speed reached the steady state, 200 rpm, after sufficient time, and there is no steady-state error. If the proportional feedback gain increases, it is seen that the response time decreases. However, the rotational speed oscillates around 200 rpm. One reason for this is an initial deformation of the rotor and the stator due to production tolerances. Another reason is that the contact conditions at each moment vary non-linearly in case of the standing wave type ultrasonic motor. The irregular oscillation of the rotational speed is caused by a summation of these reasons.

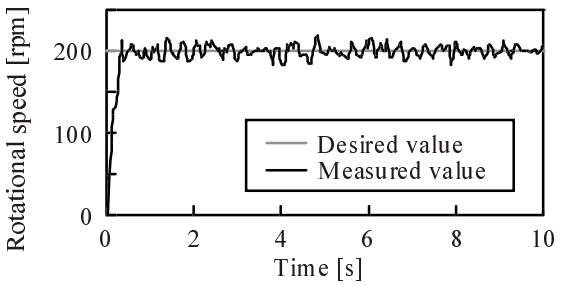

Fig. 8 Results for the speed control

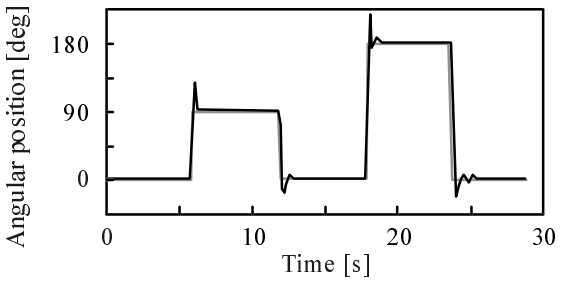

Fig. 9 Result for the position control

5.2 Experimental Results for Position Control around Single-axis

The angular position was measured when it was incrementally varied in steps. The desired angular position varied with time from 0 to 90, 0, 180 and 0 deg in order. The voltages of the input signals were the same as those in the section 5.1. The frequency was 39.94 kHz. The phase difference of the input signals was determined using the sigmoid function given in Eq. (2).

Figure 9 shows the experimental results for the step-wise response of angular position when α is 1.0 and M is 90. It can be seen from Fig. 9 that the angular position of the rotor was successfully moved to the desired position using the proposed control method. When the sigmoid function parameter α is larger than 1.0, overshoots occur. Although the proposed method is effective to control the multi-DOF ultrasonic motor, it is important to modulate the sigmoid function parameters, α and M.

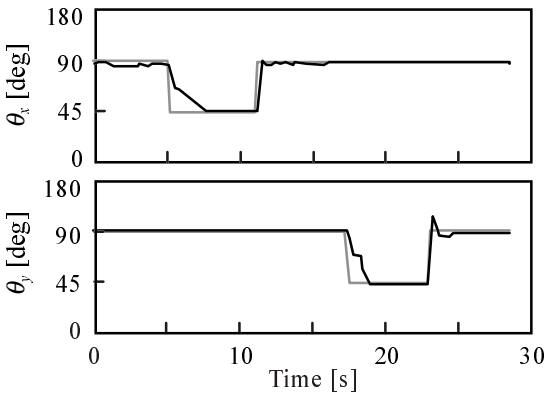

Fig. 10 Results for multi-DOF position control

5.3 Experimental Results for Multi-DOF Position Control

The position control algorithm was extended to multi-DOF position control of the spherical rotor. The desired angular positions around the *x*- and the *y*-axis were varied with time from 90 deg to 45 deg and then back to 90 deg in order. The voltages of the input signals were the same as those in the section 5.1. The frequency of the input signals was 38.90 kHz. The phase differences of the input signals were determined using the sigmoid function given in Eq. (2).

Figure 10 shows the experimental results for multi-DOF position control when α is 1 and M is 30. It can be seen from Fig. 10 that the angular positions of the spherical rotor around the *x*- and *y*-axis were successfully controlled to the desired locations.

6. CONCLUSIONS

Control methods for the multi-DOF ultrasonic motor are proposed and verified by experiments.

The driving characteristics of the multi-DOF ultrasonic motor, measured in the present work, show effects of potentially operating parameters with respect to the motion of the rotor. It is clarified in consequence that the phase difference of input signals is a suitable operating parameter for the multi-DOF ultrasonic motor. Then, control methods for the multi-DOF ultrasonic motor utilizing phase change are proposed. The motion of the multi-DOF ultrasonic motor is successfully controlled using the proposed control methods.

REFERENCES

[1] Yano, T.: Multi-DOF Actuators, *J. the Robotics Society of Japan*, Vol. 15, No. 3, pp. 330-333 (1997) [*in Japanese*]

[2] Roth, R. and Lee, K-M.: Design Optimization of a Three Degrees-of-Freedom Variable Reluctance Spherical Wrist Motor, *Trans. ASME J. Engineering for Industry*, Vol. 117, pp. 378-388 (1995)

[3] Yano, T., Suzuki, T., Sonoda, M. and Kaneko, M.: Basic Characteristics of the Developed Spherical Stepping Motor, *Proc. 1999 IEEE/RSJ Int. Conf. Intelligent Robots and Systems*, Vol. 3, pp. 1393-1398 (1999)

[4] Bansevicius, R.: Piezoelectric Multi-degree of Freedom Actuators/Sensors, *Proc. 3rd Int. Conf. Motion and Vibration Control*, pp. K9-K15 (1996)

[5] Amano, T., Ishii, T., Nakamura, K and Ueha, S.: An Ultrasonic Actuator with Multi-Degree of Freedom using Bending and Longitudinal Vibrations of a Single Stator, *Proc. IEEE Int. Ultrasonics Symp.*, pp.667-670 (1998)

[6] Toyama, S., Sugitani, S., Zhang, G., Miyatani, Y. and Nakamura, K.: Multi degree of freedom Spherical Ultrasonic Motor, *Proc. IEEE Int. Conf. Robotics and Automation*, pp. 2935-2940 (1995)

[7] Sasae, K., Ioi, K., Ohtsuki, Y. and Kurosaki, Y.: Development of a Small Actuator with Three Degrees of Rotational Freedom (3rd report), *J. Japan Society of Precision Engineering*, Vol. 62, No. 4, pp. 599-603 (1996) [*in Japanese*]

[8] Takemura, K., Maeno, T. and Kojima, N.: Development of a Bar-Shaped Ultrasonic Motor for Three-Degrees of Freedom Motion, *Proc. the 4th Int. Conf. Motion and Vibration Control*, Vol. 1, pp. 195-200 (1998)

[9] Senjyu, T., Yokoda, S., Gushiken, Y. and Uezato, K.: Position Control of Ultrasonic Motor Using Variable Structure type Adaptive Control, *Proc. IEEE 29th Annual Power Electronics Specialists Conf.*, pp. 1860-1866 (1998)

[10] Lin, F.-J., Wai, R.-J. and Duan, R.-Y.: Fuzzy Neural Networks for Identification and Control of Ultrasonic Motor Drive with LLCC Resonant Technique, *IEEE Trans. Industrial Electronics*, Vol. 46, No. 5, pp. 999-1011 (1999)

[11] Maeno, T., Tsukimoto, T. and Miyake, A.: Finite Element Analysis of the Rotor/Stator Contact in Ring-Type Ultrasonic Motor, *IEEE Trans. Ultrasonic Ferroelectrics and Frequency Control*, Vol. 39, No. 6, pp. 668-674 (1992)

[12] Maeno, T.: Contact analysis of traveling wave type ultrasonic motor considering stick/slip condition, *J. the Acoustical Society of Japan*, Vol. 54, No. 4, pp. 305-311 (1998) [*in Japanese*]

[13] Kanazawa, H., Tsukimoto T., Maeno, T. and Miyake, A.: Tribology of Ultrasonic Motors, *Tribologist*, Vol. 38, No. 3, pp. 21-26 (1993) [*in Japanese*]

APPENDIX

Sensing devices used for the experiments are shown in Fig. 11. The sensing device for single-DOF motion is illustrated in Fig. 11 (a), which can measure the angular position of the rotor around the *x*- or *y*-axis. The sensing device for multi-DOF motion is illustrated in Fig. 11 (b), which can measure the angular positions of the rotor around the *x*- and *y*-axis.

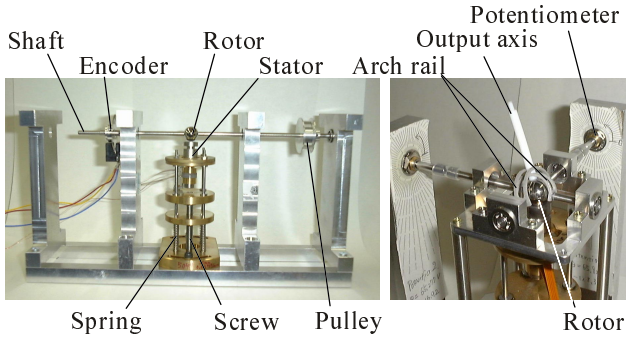

(a) Single-DOF motion (b) Multi-DOF motion

Fig. 11 Developed sensing devices